Sarag J. Saikia[1]
School of Aeronautics and Astronautics,
Purdue University,
701 West Stadium Avenue,
West Lafayette, IN 47907-2045
e-mail: sarag@purdue.edu

Jeffrey F. Rhoads
Fellow ASME
Associate Professor
School of Mechanical Engineering,
Purdue University,
585 Purdue Mall,
West Lafayette, IN 47907-2088
e-mail: jfrhoads@purdue.edu

James M. Longuski
Professor
School of Aeronautics and Astronautics,
Purdue University,
701 West Stadium Avenue,
West Lafayette, IN 47907-2045
e-mail: longuski@purdue.edu

Improved Perturbative Solution of Yaroshevskii's Planetary Entry Equation

An improved approximate analytical solution is developed for Yaroshevskii's classical planetary entry equation for the ballistic entry of a spacecraft into planetary atmospheres at circular speed. Poincaré's method of small parameters is used to solve for the altitude and flight path angle as a function of the spacecraft's speed. From this solution, other important expressions are developed including deceleration, stagnation-point heat rate, and stagnation-point integrated heat load. The accuracy of the solution is assessed via numerical integration of the exact equations of motion. The solution is also compared to the classical solutions of Yaroshevskii and Allen and Eggers. The new second-order analytical solution is more accurate than Yaroshevskii's fifth-order solution for a range of shallow (−3 deg) to steep (up to −90 deg) entry flight path angles, thereby extending the range of applicability of the solution as compared to the classical Yaroshevskii solution, which is restricted to an entry flight path of approximately −40 deg.
[DOI: 10.1115/1.4033553]

1 Introduction

The flight of an aerospace vehicle in a planetary atmosphere involves highly nonlinear dynamics, which makes the development of closed-form solutions a challenging problem. Over the course of entry and descent, a spacecraft is subjected to a wide range of atmospheric forces beginning with the barely sensible atmospheric drag (which is negligible compared to the gravitational force) to very large aerodynamic forces (which are an order of magnitude greater than the gravitational force). The nonlinearities in the equations of motion of an aerospace vehicle in a planetary atmosphere are due to the inverse square Newtonian gravity, aerodynamic forces (a function of drag coefficient, density, and the square of the velocity), and the appearance of trigonometric terms. For example, consider the entry of a spacecraft at Earth; the density (a function of altitude) of the atmosphere changes from an order of about $10^{-8}\,\mathrm{kg/m^3}$ at entry interface (at an altitude of about 120 km) to about $1.2\,\mathrm{kg/m^3}$ near the planetary surface.

Most of the early analytical work to understand the motion of ballistic missiles and spacecraft inside a planetary atmosphere was carried out in the 1950 s, 1960 s, and the 1970 s. Along with the needs of missile programs, the American and Russian space programs stimulated the desire for analytical work particularly when fast computational tools were in their nascent stage of development. Currently, there is a renewed interest in analytical theories for spacecraft entry as the analytical solutions for various entry problems may aid in the rapid conceptual design of entry spacecraft for planetary exploration missions. Though it is not the part of the analysis presented in this paper, the analytical solutions can also provide initial guesses for the optimization subroutines used to solve complex spacecraft entry and hypersonic flight problems.

In general, the equations governing the motion of a spacecraft entering a planetary atmosphere do not have closed-form analytical solutions. For restrictive regions of application, several first- and second-order approximate analytical solutions for entry problems with ballistic and constant lift-to-drag ratios have been obtained in the past. Sänger and Bredt [1] and Gazley [2], for example, obtained analytical solutions for ballistic entry into an atmosphere. For strategic applications and using simplified assumptions, Allen and Eggers [3] developed closed-form analytical solutions for the entry of ballistic missiles that minimize heating. Loh found generalized solutions for (a) ballistic entry and (b) for a wide range of lift-to-drag ratios, for various initial flight path angles [4–6]. The formulation of Loh's theory was done based on empirical data obtained from the extensive integration of entry trajectories for a variety of ballistic coefficients, initial velocities, and entry flight path angles. Chapman derived a generalized second-order nonlinear differential equation, free of vehicle characteristics and applicable to any lift-to-drag ratio [7]. In the general case, numerical integration of Chapman's equation is required to obtain the solution of planetary entry. Longuski and Saikia developed a new and improved analytical theory for spacecraft ballistic entry at circular speed for the entire range of initial flight path angles where Yaroshevskii's solution appears as the zero-order term [8]. Longuski and Saikia formulated a second theory which is applicable for spacecraft ballistic entry at any entry speed for moderate to large entry flight path angles [9–11]. Vinh et al. developed a set of exact universal entry equations applicable to spacecraft in all regimes of flight—from orbital motion, entry phase, glide, and touchdown [12]. The universal equations are valid for all types of entry vehicles—regardless of mass, size, and aerodynamic characteristics. Vinh and Brace removed Chapman's restrictive assumptions to modify the generalized system of equations [13]. The doctoral dissertations of Brace [14] and Blestos [15] validate the advantage of the generalized equations of motion.

In 1964, Yaroshevskii developed a generalized semi-analytical entry theory which is of interest in this paper [16,17]. Yaroshevskii's theory is generalized in the sense that it allows a single trajectory solution for a given initial velocity and flight path angle to be computed which applies to every possible ballistic spacecraft, regardless of the mass, surface area, and drag coefficient.

[1]Corresponding author.

Contributed by the Design Engineering Division of ASME for publication in the Journal of Computational and Nonlinear Dynamics. Manuscript received December 24, 2014; final manuscript received April 18, 2016; published online June 7, 2016. Assoc. Editor: Haiyan Hu.

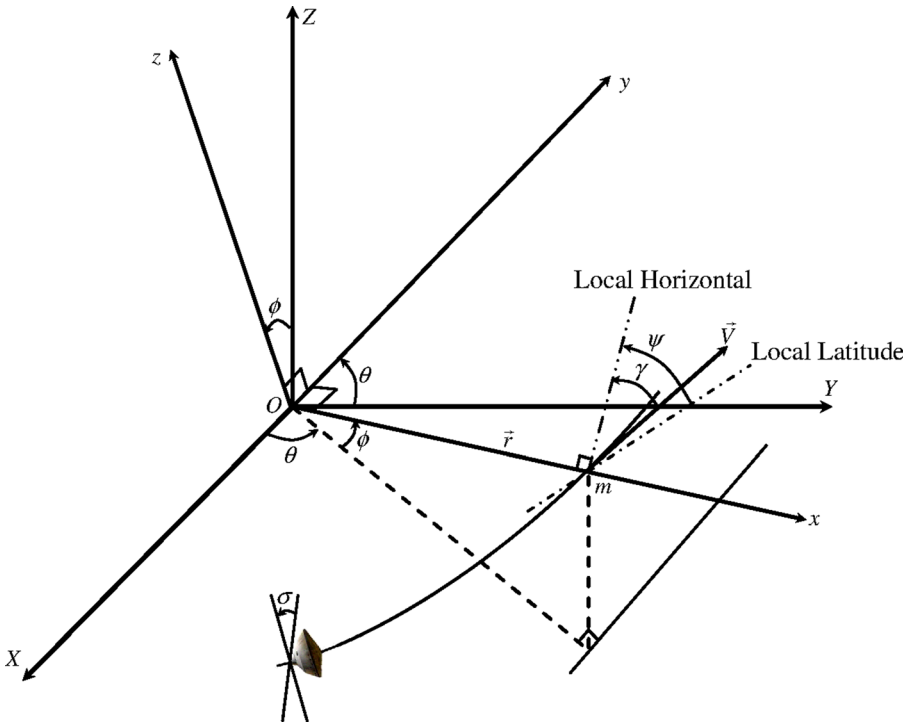

Fig. 1 Coordinate systems for the three-degree-of-freedom motion of a spacecraft inside a planet's atmosphere. Adapted from Ref. [12].

Yaroshevskii demonstrated that when the tangential gravitational acceleration is neglected, the planar equations of entry can be transformed to a second-order nonlinear ordinary differential equation which can be integrated analytically (via series expansion) for the case of entry at circular speed for zero and small initial flight path angles. Separate solutions are available for both ballistic and lifting (limited to small lift-to-drag coefficients) entry. It was found that Yaroshevskii's theory is a distinct case of the more refined theory of Chapman [12].

In this paper, Poincaré's method of small parameters is used to solve Yaroshevskii's second-order nonlinear differential equation for ballistic entry at circular speed for nonzero initial flight angles. We then assess the accuracy of both the first- and second-order solutions by comparing them to results obtained by numerically integrating the original equations of motion. The new approximate analytical solution is then compared with the classical solutions of Yaroshevskii and Allen and Eggers.

2 Planetary Entry Equations of Motion

We consider the flight of a nonthrusting, lifting spacecraft of mass m inside the atmosphere of a planetary body. The spacecraft is modeled as a point mass and the rotations of the planetary body as well as its atmosphere are neglected. A universal gravitational field is also assumed. The effects of perturbations due to a planet's oblateness (e.g., J_2) are small enough that they can be neglected due to the relatively short timeline of spacecraft entry. The planet's rotation and accompanying effects on wind-relative velocity represent a steady source of error which can be reduced by using the velocity relative to the planet.

The $OXYZ$ reference frame is fixed with respect to the planetary body. Therefore, the $OXYZ$ is rotating with an angular velocity (assumed to be constant) acting along the Z-axis. The position vector, $\mathbf{r}$, is defined by its magnitude, r. The longitude, θ, is defined in the equatorial plane, measured from the X-axis, positively, eastward. The latitude, ϕ, is measured from the equatorial plane and measured positively northward. In addition, the other trajectory variables are: planet-centric velocity magnitude, V, flight path angle, γ, relative to the local horizontal, and the heading angle, ψ, relative to the local latitude line. A rotating coordinate system, $Oxyz$, has been found to be more convenient, as it is easier to evaluate different vectors (in the planet-centric frame) using their components in the $Oxyz$ frame [10].

The bank angle, σ, is defined as the angle between the local vertical plane (containing $\mathbf{r}$ and V) and the lift vector. The coordinate systems and variables that describe the three-degree-of-freedom motion of a spacecraft inside a planet's atmosphere are shown in Fig. 1. Given the assumptions, the three-degree-of-freedom equations of motion are

$$\frac{dr}{dt} = V\sin\gamma \tag{1}$$

$$\frac{d\theta}{dt} = \frac{V\cos\gamma\cos\psi}{r\cos\phi} \tag{2}$$

$$\frac{d\phi}{dt} = \frac{V\cos\gamma\sin\psi}{r} \tag{3}$$

$$\frac{dV}{dt} = -\frac{\rho S C_D V^2}{2m} - g\sin\gamma \tag{4}$$

$$V\frac{d\gamma}{dt} = \frac{\rho S C_L V^2}{2m}\cos\sigma - \left(g - \frac{V^2}{r}\right)\cos\gamma \tag{5}$$

$$\frac{d\psi}{dt} = \frac{\rho S C_L V^2}{2m}\sin\sigma - \frac{V^2}{r}\cos\gamma\cos\psi\tan\phi \tag{6}$$

The constant g in Eqs. (4) and (5) refers to the local gravitational acceleration of a given planet. The constant S is the reference area, and C_L and C_D are the lift and drag coefficients of the entry spacecraft, respectively. The atmosphere is assumed to be strictly exponential and is governed by

$$\frac{d\rho}{\rho} = -\beta dr \tag{7}$$

In the strictly exponential atmosphere model, the inverse of atmospheric scale height, β, is considered constant.

In general, the original equations of motion given by Eqs. (1)–(6) are not suitable for finding closed-form solutions. However, with a judicious choice of variables, the equations of motion can be transformed into a tractable form to yield an analytical solution.

3 Yaroshevskii's Entry Equation of Motion and Modeling Assumptions

For ballistic trajectories in the absence of lift, an entry spacecraft's motion is planar. The planar equations of motion are given by Eqs. (1), (4), and (5) with $C_L = 0$. In this paper, we will be concerned with the case of ballistic entry at circular speed for nonzero initial flight path angles. In general, the lift and the drag coefficients of spacecraft, C_L and C_D, are functions of the angle of attack, α, Mach number M, and the Reynolds number, Re. For constant angle of attack, Yaroshevskii assumed that C_L and C_D are functions of the Mach number. For an isothermal atmosphere, C_L and C_D are functions of speed, V [12]. Due to the Mach number independence in the hypersonic flight regime (as in the case of an entry spacecraft), the assumption of constant aerodynamic coefficients, C_L and C_D, is valid for a major portion of entry trajectories. We note that the solution of Yaroshevskii's entry equation of motion is also applicable to the entry of any vehicle at any speed less than circular speed (e.g., re-entry of a ballistic missile).

For ballistic entry, the tangential gravitational acceleration, given by $g\sin\gamma$, is very small as compared to the drag acceleration, and hence can be neglected. Yaroshevskii also assumed a small flight path angle so that

$$\sin\gamma \approx \gamma \text{ and } \cos\gamma \approx 1 \tag{8}$$

Neglecting the tangential gravitational acceleration and with a small flight path angle approximation, the planar entry equations of motion given by Eqs. (1), (4), and (5) become

$$\frac{dr}{dt} = V\gamma \tag{9}$$

$$\frac{dV}{dt} = -\frac{\rho S C_D V^2}{2m} \tag{10}$$

$$V\frac{d\gamma}{dt} = \frac{\rho S C_L V^2}{2m} - \left(g - \frac{V^2}{r}\right) \tag{11}$$

To change the independent variable from time, t, to the velocity, V, we divide Eqs. (9) and (11) by Eq. (10) to get the new planar entry equations of motion

$$\frac{dr}{dV} = -\frac{2m\gamma}{\rho S C_D V} \tag{12}$$

$$V\frac{d\gamma}{dV} = -\frac{C_L}{C_D} + \frac{2m\left(g - \frac{V^2}{r}\right)}{\rho S C_D V^2} \tag{13}$$

For the critical phase of spacecraft entry where the Mach number is very high, the lift and drag coefficients, C_L and C_D, are independent of the Mach number, M. By considering C_L and C_D as constants, Yaroshevskii defined the independent velocity variable, x, and dependent altitude variable, y, as follows [12]:

$$x \equiv -\int_1^{\bar{V}} \frac{d\bar{V}}{\bar{V}} \tag{14}$$

$$y \equiv \frac{SC_D}{2m}\sqrt{\frac{r_0}{\beta}}\rho \tag{15}$$

where r_0 is the radius of the planet and $\bar{V}$ is dimensionless speed. In general, the altitude, h, can be considered very small as compared to the radius of the planet, r_0, such that the term $\sqrt{gr_0}$ is equivalent to the circular speed at entry interface. Therefore, the dimensionless speed variable is given by

$$\bar{V} \equiv \frac{V}{\sqrt{gr_0}} \tag{16}$$

From the definition of strictly exponential atmosphere in Eq. (7), given the dependent altitude variable, y, we also get

$$\frac{dy}{y} = -\beta dr \tag{17}$$

By neglecting the altitude, h, as compared to the radius of the planet, r_0, and using the definitions in Eqs. (14)–(16) in Eqs. (12) and (13), the transformed equations of motion are

$$\frac{dy}{dx} = \Phi = -\sqrt{\beta r_0}\,\gamma \tag{18}$$

$$\frac{d\gamma}{dx} = \frac{C_L}{C_D} - \frac{1-\bar{V}^2}{\sqrt{\beta r_0}\,y\bar{V}^2} \tag{19}$$

where Φ in Eq. (18) is the new flight path angle variable.

Using Eq. (18) in Eq. (19) to eliminate the flight path angle, γ, we obtain

$$\frac{d^2y}{dx^2} = -\sqrt{\beta r_0}\frac{C_L}{C_D} + \frac{\bar{V}^{-2} - 1}{y} \tag{20}$$

As defined earlier, here the Mach number is very high, and the lift and drag coefficients, C_L and C_D, are independent of the Mach number, M. Therefore, the independent velocity variable is given by

$$x = \ln\left(\frac{\sqrt{gr_0}}{V}\right) \tag{21}$$

$$\bar{V} = e^{-x} \tag{22}$$

We note that in Eq. (21), any entry speed greater than the circular speed $\sqrt{gr_0}$ makes the initial value of the independent velocity variable, x, negative. This fact places a constraint on the applicability of Yaroshevskii's planetary entry theory to entry speed equal to or less than the circular speed. Using the results in Eqs. (21) and (22) in Eq. (20), we get a single second-order equation of the planar lifting entry of spacecraft given by

$$\frac{d^2y}{dx^2} = -\sqrt{\beta r_0}\frac{C_L}{C_D} + \frac{e^{2x} - 1}{y} \tag{23}$$

where the term βr_0 is constant for altitudes below 120 km. The mean value of βr_0 is large, varying from a minimum of about 750 to a maximum of 1300. In general, it is a standard practice to consider an average value of $\beta r_0 = 900$ for Earth. Equation (23), first derived by Yaroshevskii, is a second-order nonlinear ordinary differential equation that describes the planar motion of a spacecraft entering a planetary atmosphere [12,16,17]. If Eq. (23) is solved, then the altitude variable, y, can be expressed as a function of independent variable, x, and all the other trajectory parameters of interest can be computed thereafter.

4 Summary of Classical Solution of Yaroshevskii's Equation for Ballistic Entry

Yaroshevskii obtained two separate analytical solutions for ballistic entry at circular speed—one for zero initial flight path angle and the second for various values of nonzero initial flight path angles. Ballistic entry at zero initial flight path angles has limited applications. Therefore, we are concerned about the ballistic entry at circular speed for nonzero initial flight path angles. To obtain Yaroshevskii's equation for the ballistic entry of a spacecraft into planetary atmosphere, we substitute $(C_L/C_D) = 0$ in Eq. (23) to obtain

$$\frac{d^2y}{dx^2} = \frac{e^{2x} - 1}{y} \tag{24}$$

Although Eq. (24) looks simple, it turns out that it is not separable.

4.1 Ballistic Entry at Circular Speed for Entry at Nonzero Initial Flight Path Angles. When the initial flight path angle is nonzero, the nonlinear differential equation can be integrated for circular orbits. For entry from circular orbits, using Eq. (4), the initial conditions are

$$x_i = 0 \tag{25}$$

$$y(0) \approx 0 \tag{26}$$

$$y'(0) = \phi_i = c_1 = -\sqrt{\beta r_0}\,\gamma_i \tag{27}$$

Yaroshevskii found a series solution of the form for the altitude variable, y, in terms of the independent velocity variable, x

$$y = \sum_{k=1}^{\infty} c_k x^k \tag{28}$$

where c_k are the coefficients of the terms in the series on the right-hand side of Eq. (28). The value of k is judiciously selected such that $k \geq 1$. This is because when Eq. (28) is used in Eq. (24) such that yy'' is equated to $(e^{2x} - 1)$, then $c_0 = 0$, as there is no constant term in the expression $(e^{2x} - 1)$.

Rewriting Eq. (28), we have

$$y = c_1 x + c_2 x^2 + c_3 x^3 + c_4 x^4 + c_5 x^5 + \cdots \tag{29}$$

and from Eq. (18), the flight path angle variable is given by

$$\Phi = \frac{dy}{dx} = c_1 + 2c_2 x + 3c_3 x^2 + 4c_4 x^3 + 5c_5 x^4 + \cdots \tag{30}$$

By substituting Eq. (28) into Eq. (24) and equating the coefficients of like powers in x, we obtain the c_k coefficients

$$c_0 = 0 \tag{31}$$

$$c_2 = \frac{1}{c_1} \tag{32}$$

$$c_3 = \left(1 - \frac{1}{c_1^2}\right)\frac{1}{3c_1} \tag{33}$$

$$c_4 = \left(1 - \frac{2}{c_1^2} + \frac{2}{c_1^4}\right)\frac{1}{9c_1} \tag{34}$$

$$c_5 = \left(3 - \frac{10}{c_1^2} + \frac{20}{c_1^4} - \frac{17}{c_1^6}\right)\frac{1}{90c_1} \tag{35}$$

Yaroshevskii found the general expression for the coefficients of the series in Eq. (28), which is given by

$$c_1 c_k = \frac{2^{k-1}}{k(k-1)(k-1)!} - \sum_{q=2}^{k-1} q(q-1)c_q c_{k+1-q} \tag{36}$$

Therefore, using Eqs. (31)–(35) or in general Eq. (36) in Eqs. (29) and (30), the altitude and flight path angle variables can be expressed as functions of the independent velocity variable. From these variables, the physical variables of altitude, flight path angle, and velocity, as well as important aerodynamic heating parameters, can be readily obtained.

5 New Perturbative Solution for Yaroshevskii's Entry Equation

In this section, we use Poincaré's method of small parameters (also known as the Poincaré–Lindstedt method) to solve the differential equation governing the ballistic entry of spacecraft at circular speed for nonzero initial flight path angles. The independent variable, x, monotonically increases for all the possible atmospheric entry trajectory cases—direct entry, aerocapture, and fly-through. In order to use Poincaré's method of small parameters, we artificially insert a small parameter defined by

$$\varepsilon = y(0) = \frac{C_D S}{2m}\sqrt{\frac{r_0}{\beta}}\rho_e \tag{37}$$

The parameter is of the order 10^{-5}. We also introduce the following new altitude variable, η, and independent velocity variable, τ, which are functions of the original variables y and x :

$$\eta \equiv \frac{y}{\varepsilon} \tag{38}$$

$$\tau \equiv \frac{x}{\varepsilon} \tag{39}$$

such that the following two differential relations hold:

$$\frac{d\tau}{dx} = \frac{1}{\varepsilon} \tag{40}$$

$$\frac{d()}{d\tau} = ()' \tag{41}$$

Using Eqs. (38) and (39) in Eq. (24), the transformed Yaroshevskii equation for ballistic entry into planetary atmosphere is given by

$$\frac{d^2\eta}{d\tau^2} = \frac{e^{2\varepsilon\tau} - 1}{\eta} \tag{42}$$

With the appearance of the small parameter, ε, Eq. (42) is in an appropriate form for the application of Poincaré's method of small parameters. Therefore, we seek a solution of the form

$$\eta = \eta_0 + \varepsilon\eta_1 + \varepsilon^2\eta_2 + \cdots \tag{43}$$

The initial conditions for the nonlinear differential equations in Eq. (42) are given by

$$\eta_0(0) = 1 \tag{44}$$

$$\eta_1(0) = \eta_2(0) = \cdots = 0 \tag{45}$$

$$\eta_0'(0) = -\sqrt{\beta r_0}\sin\gamma_i = b \tag{46}$$

$$\eta_1'(0) = \eta_2'(0) = \cdots = 0 \tag{47}$$

We substitute Eq. (43) into Eq. (42) and expand the exponential series, $e^{2\tau\varepsilon}$. In the resulting equation, by equating the coefficients of different powers of ε, and after some algebra, the following system of equations are obtained:

$$\varepsilon^0: \quad \eta_0'' = 0 \tag{48}$$

$$\varepsilon^1: \quad \eta_1'' - \frac{2\tau}{\eta_0} = 0 \tag{49}$$

$$\varepsilon^2: \quad \eta_2'' + \frac{2\eta_1\tau}{\eta_0^2} - \frac{2\tau^2}{\eta_0} = 0 \tag{50}$$

The equation only up to the second power of ε, i.e., ε^2, is retained corresponding to the second-order solutions. Equations (48)–(50) must be sequentially solved. Using the initial conditions in Eqs. (44) and (45), the solution of Eq. (48) is given by

$$\eta_0 = b\tau + a \tag{51}$$

Using the result from Eq. (51) in the first-order equation of η, Eq. (49), and by using the initial condition in Eqs. (45) and (47), the solution of the first-order term is given by

$$\eta_1 = \frac{1}{b^3}[b\tau(b\tau+2) - 2(b\tau+1)\ln(b\tau+1)] \tag{52}$$

By substituting Eqs. (51) and (52) in the second-order equation, Eq. (50), and by using the initial condition in Eqs. (45) and (47), the solution is given by

$$\begin{aligned}\eta_2 = &-\frac{1}{3b^6}[-b^5\tau^3 + 3b^4\tau^2 + b^3\tau(\tau^2+15) + 9b^2\tau^2] \\ &+ \frac{2\tau\ln(b\tau+1)}{b^3} + \frac{2(\tau^2+1)\ln(b\tau+1)}{b^4} + \frac{5(b\tau+1)}{3b^6} \\ &- \frac{2(b\tau+1)[\ln(b\tau+1)]^2}{b^6} - \frac{11\tau}{b^5} - \frac{4}{b^6}\end{aligned} \tag{53}$$

Using the results in Eqs. (51)–(53), solutions of different orders can be constructed. The first-order solution of the altitude variable, η, is given by

$$\eta = \eta_0 + \varepsilon\eta_1 \tag{54}$$

Substituting the results in Eqs. (51) and (52) into Eq. (54) yields the first-order solution

$$\eta = (b\tau + a) + \frac{\varepsilon}{b^3}[b\tau(b\tau+2) - 2(b\tau+1)\ln(b\tau+1)] \tag{55}$$

The second-order solution of the altitude variable, η, is given by

$$\eta = \eta_0 + \varepsilon\eta_1 + \varepsilon^2\eta_2 \tag{56}$$

Using the results in Eqs. (51)–(53), the complete second-order solution of the altitude variable, η, is given by

$$\begin{aligned}\eta = &(b\tau + a) + \frac{\varepsilon}{b^3}[b\tau(b\tau+2) - 2(b\tau+1)\ln(b\tau+1)] \\ &- \frac{\varepsilon^2}{3b^6}[-b^5\tau^3 + 3b^4\tau^2] - \frac{\tau\varepsilon^2(\tau^2+15)}{3b^3} - \frac{3(\varepsilon\tau)^2}{3b^4} \\ &+ \frac{\varepsilon^2}{b^6}\{2\ln(b\tau+1)[b^3\tau + b^2(\tau^2+1) + 5(b\tau+1)]\} \\ &- \frac{2\varepsilon^2(b\tau+1)[\ln(b\tau+1)]^2}{b^6} - \frac{11\tau\varepsilon^2}{b^5} - \frac{4\varepsilon^2}{b^6}\end{aligned} \tag{57}$$

We note that only first- and second-order solutions are summarized in Eqs. (55) and (57). The zero-order is not highlighted as we see that it is a straight line defined by Eq. (51).

We now find the flight path angle in terms of the new variables, η and τ, using the definitions of the variables, η and τ, in Eqs. (38) and (39)

$$\Phi = -\sqrt{\beta r_0}\,\gamma = \frac{d\eta}{d\tau} \tag{58}$$

The first-order solution of the flight path angle variable, Φ, in terms of the new variables, η and τ, is given by

$$\Phi = \frac{d\eta_0}{d\tau} + \varepsilon\frac{d\eta_1}{d\tau} \tag{59}$$

Differentiating Eqs. (51)–(53) with respect to the independent velocity variable, and substituting the results into Eq. (59), we obtain the first-order solution of the flight path angle variable as follows:

$$\Phi = b + \frac{2\varepsilon}{b^2}[b\tau - \ln(b\tau+1)] \tag{60}$$

Similarly, the second-order solution of the flight path angle variable, Φ, in terms of the new variables, η and τ, is given by

$$\Phi = \frac{d\eta_0}{d\tau} + \varepsilon\frac{d\eta_1}{d\tau} + \varepsilon^2\frac{d\eta_2}{d\tau} \tag{61}$$

Differentiating Eqs. (51)–(53) with respect to the independent velocity variable, τ, and substituting the results into Eq. (61), we obtain the second-order solution of the flight path angle variable as follows:

$$\begin{aligned}\Phi = &b + \frac{2\varepsilon}{b^2}[b\tau - \ln(b\tau+1)] - \frac{\varepsilon^2}{b^6}(11b + 5b^3) \\ &- \frac{\varepsilon^2}{b^3}[2b\tau - (1-b^2)\tau^2] - \frac{2\varepsilon^2}{b^5}\frac{(b^2+5)}{b\tau+1} \\ &- \frac{2\varepsilon^2}{b^5}(b^2+5)\ln(b\tau+1) - \frac{2\varepsilon^2}{b^4}\frac{(b^2+5)\tau}{b\tau+1} \\ &- \frac{4\varepsilon^2}{b^4}\tau\ln(b\tau+1) - \frac{2\varepsilon^2}{b^3}\frac{\tau^2}{b\tau+1} - \frac{5\varepsilon^2}{b^5}\frac{\ln(b\tau+1)}{(b\tau+1)} \\ &- \frac{2\varepsilon^2}{b^5}[\ln(b\tau+1)]^2 - \frac{4\varepsilon^2}{b^4}\frac{\tau\ln(b\tau+1)}{b\tau+1}\end{aligned} \tag{62}$$

The constant b is defined by the planetary atmosphere through the term $\sqrt{\beta r_0}$ and the value of the flight path angle at entry interface, γ_i. Equations (55) and (57) represent the first- and second-order solutions of the altitude variable, η. Similarly, Eqs. (60) and (62) represent the first- and second-order solutions of the flight path angle variable, Φ. We again note that the constant b is defined by Eq. (46). The solutions of the altitude variable, η, flight path angle variable, Φ, and the independent velocity variable, τ, represent the ballistic planar motion of a spacecraft inside a planetary atmosphere. From the basic structure of the solutions and the way the constant b appears, it is evident that the solutions are valid only for nonzero values of initial flight path angle. At first sight, the perturbative solutions of the altitude variable, η, and flight path angle variable, Φ, might look complicated. However, it is notable that the terms in the solutions are simple mathematical functions of the constant b and the independent variable τ. In the Results and Discussion section, we will analyze the range of initial flight path angles for which the solution is valid. We know that the use of up to fourth-order terms in Yaroshevskii's solution is required in the approximate series solution to achieve the accuracy required to cover the regime where the key events such as the peak deceleration and peak heating occur. However, for the new

perturbative solution, only up to first-order terms are required to attain a similar or better level of accuracy of the series solution.

6 Trajectory Parameters and Aerodynamic Heating Expressions

In this section, we use the solution in dimensionless variables to find the trajectory parameters (altitude, flight path angle, and velocity) and important aerodynamic heating expressions.

6.1 Velocity. For Yaroshevskii's variables, the velocity can be obtained from Eq. (22)

$$V = \sqrt{gr_0}\, e^{-x} \tag{63}$$

Substituting the new perturbative variables definition from Eqs. (38) and (39) in Eq. (63)

$$V = \sqrt{gr_0}\, e^{-\varepsilon\tau} \tag{64}$$

6.2 Altitude. To find the altitude, we recall the definition of Yaroshevskii's altitude variable

$$y \equiv \frac{SC_D}{2m}\sqrt{\frac{r_0}{\beta}}\rho \tag{65}$$

From Eq. (65), the altitude can be obtained via the following equation:

$$h = h_0 - \frac{1}{\beta}\ln\left(\frac{y}{y_0}\right) \tag{66}$$

where h_0 is the value of the altitude at entry interface. The variable y_0 is the value of the altitude variable given by

$$y_0 \equiv \frac{SC_D}{2m}\sqrt{\frac{r_0}{\beta}}\rho_e \tag{67}$$

where ρ_e is the value of the atmospheric density at entry interface.

6.3 Flight Path Angle. From Eqs. (18) and (58), the flight path angle variable, Φ, in terms of both Yaroshevskii's and the new perturbative variable is given by

$$\Phi = \frac{dy}{dx} = \frac{d\eta}{d\tau} \tag{68}$$

Therefore, the flight path angle for Yaroshevskii's case is given by

$$\gamma = -\frac{1}{\sqrt{\beta r_0}}\left(\frac{dy}{dx}\right) \tag{69}$$

where y represents of the classical solution of Yaroshevskii's equation given by Eq. (29).

The flight path angle in terms of the new perturbative variables is given by

$$\gamma = -\frac{1}{\sqrt{\beta r_0}}\left(\frac{d\eta}{d\tau}\right) \tag{70}$$

where the first- and second-order expressions for $d\eta/d\tau$ are given by Eqs. (60) and (62), respectively.

6.4 Time of Flight. To compute the time of flight of the spacecraft inside a planetary atmosphere, we use the definitions of the Yaroshevskii's altitude and velocity variables. Substituting Eqs. (15) and (21) into Eq. (10), we obtain

$$\frac{dx}{dt} = \sqrt{\beta g}\, y\, e^{-x} \tag{71}$$

Equation (71) can be rearranged and integrated from time $(t = 0)$ at entry interface to any time t, to yield the expression for the time of flight

$$t = \frac{1}{\sqrt{\beta g}}\int_{x_i}^{x}\frac{e^x}{y}\,dx \tag{72}$$

Using the definition of the new perturbative variables from Eqs. (38) and (39) in Eq. (71), we obtain

$$\frac{d\tau}{dt} = \sqrt{\beta g}\,\eta\, e^{-\tau\varepsilon} \tag{73}$$

Again, by rearranging and integrating, we obtain the expression for the time of flight in terms of the new perturbative variables

$$t = \frac{1}{\sqrt{\beta g}}\int_{\tau_i}^{\tau}\frac{e^{\tau\varepsilon}}{\eta}\,d\tau \tag{74}$$

6.5 Range. The expression of range could be useful for onboard guidance and spacecraft targeting systems. The distance traveled by a spacecraft inside a planetary atmosphere is governed by

$$\frac{ds}{dt} = \frac{r_0}{r}\, V\cos\gamma \tag{75}$$

For a small flight path angle approximation, and by assuming that the radius, r, of the spacecraft's trajectory is comparable to the radius of the planet, r_0, and using Eq. (21), Eq. (71) becomes

$$\frac{ds}{dt} = \sqrt{gr_0}\, e^{-x} \tag{76}$$

We substitute the expression for the differential, dt, from Eq. (71) into Eq. (72) and after integration within the limits, we obtain the equation for range

$$s = \sqrt{\frac{r_0}{\beta}}\int_{x_i}^{x}\frac{dx}{y} \tag{77}$$

where y is an approximate power series of the velocity variable, x, given by Eq. (29). Similarly, the range in terms of the new perturbative variables is given by

$$s = \sqrt{\frac{r_0}{\beta}}\int_{\tau_i}^{\tau}\frac{d\tau}{\eta} \tag{78}$$

6.6 Deceleration. The deceleration, G, of the spacecraft along its trajectory, in Earth g's, is obtained from the force equation, Eq. (10)

$$G = -\frac{(dV/dt)}{g} = \frac{\rho SC_D}{2mg}V^2 \tag{79}$$

Rearranging Eq. (79) and using Eqs. (15) and (21), we obtain the relation for deceleration in terms of Yaroshevskii's variables, y and x

$$G = \sqrt{\beta r_0}\, y\, e^{-2x} \tag{80}$$

Using the definitions in Eqs. (38) and (39), the deceleration in terms of the new perturbative variables is given by

$$G = \sqrt{\beta r_0 \varepsilon^2}\ \eta\, e^{-2\tau\varepsilon} \tag{81}$$

6.7 Stagnation-Point Heating Rate. The stagnation-point heating rate is a function of the vehicle shape, atmospheric properties, and entry interface conditions. The value of the stagnation-point heating rate determines the type of the thermal protection system used on a spacecraft entering a planetary atmosphere. Since Yaroshevskii's theory is applicable to any entry speed equal to or less than the circular, we are concerned about only the convective stagnation-point heating rate. Only for higher entry speeds, such as for lunar return trajectories or hyperbolic entries, does radiative heating become significant so that it can no longer be neglected. The local convective stagnation-point heating rate of an entry spacecraft is given by

$$Q_s = \frac{C}{\sqrt{R_n}}\sqrt{\rho}\, V^3 \tag{82}$$

where C is the stagnation-point heating coefficient which varies according to the planet and the entry vehicle shape and size. For Earth, $C = 2.85 \times 10^{-8}$ kg$^{1/2}$ m^{-1}. The variable R_n is the nose radius of an entry spacecraft which characterizes how blunt a spacecraft is. The larger the nose radius, the blunter the spacecraft, and consequently, the smaller the stagnation-point heating rate. The stagnation-point heating rate is expressed in W/cm^2.

The local convective stagnation-point heating rate in terms of Yaroshevskii's variables is given by

$$Q_s = \frac{C}{\sqrt{R_n}}\left(\frac{\beta}{r_0}\right)^{\frac{1}{4}}\left(\frac{2m}{SC_D}\right)^{\frac{1}{2}}\sqrt{y}\, e^{-3x} \tag{83}$$

The local convective stagnation-point heating rate in terms of the new perturbative variables is given by

$$Q_s = \frac{C}{\sqrt{R_n}}\left(\frac{\beta}{r_0}\right)^{\frac{1}{4}}\left(\frac{2m\varepsilon}{SC_D}\right)^{\frac{1}{2}}\sqrt{\eta}\, e^{-3\tau\varepsilon} \tag{84}$$

6.8 Total Stagnation-Point Heat Load. The total stagnation-point heat load is obtained through the integration of the stagnation-point heating rate from entry interface to landing. The total heat load determines the mass of the thermal protection system that needs to be used on an entry spacecraft. Therefore, in general, the total stagnation-point heat load Q_t is given by the equation

$$Q_t = \frac{C}{\sqrt{R_n}}\int_0^t \sqrt{\rho}\, V^3 dt \tag{85}$$

The total convective stagnation-point heat load in terms of Yaroshevskii's variables is given by

$$Q_t = \frac{C}{\sqrt{R_n}}\left(\frac{2m}{SC_D}\right)^{\frac{1}{2}}\left(\frac{\beta}{r_0}\right)^{\frac{1}{2}}\left(\frac{1}{gr_0}\right)^{\frac{1}{2}}\int_{x_i}^{x}\frac{e^{-2x}}{y}dx \tag{86}$$

The total convective stagnation-point heat load in terms of the new perturbative variables is given by

$$Q_t = \frac{C}{\sqrt{R_n}}\left(\frac{2m}{SC_D}\right)^{\frac{1}{2}}\left(\frac{\beta}{r_0}\right)^{\frac{1}{2}}\left(\frac{1}{gr_0}\right)^{\frac{1}{2}}\int_{\tau_i}^{\tau}\frac{e^{-2\tau\varepsilon}}{\eta}\, d\tau \tag{87}$$

7 Brief Summary of Allen–Eggers Solutions for Planar Ballistic Entry

Allen and Eggers developed a theory for spacecraft planar ballistic entry into a planetary atmosphere [3]. Allen–Eggers assumed that the tangential gravitational acceleration, $g\sin\gamma$, is very small compared to the drag acceleration for both steep and shallow entries. For shallow entries, the tangential gravitational acceleration is small owing to the small values of the flight path angles (hence, small $\sin\gamma$). This assumption of the Allen–Eggers entry theory is the same as in the case of Yaroshevskii's theory. Allen–Eggers' theory differs from Yaroshevskii's theory in the simplified assumption for the flight path angle. In Allen–Eggers theory, the flight path angle is assumed to remain constant at the value of the entry flight path angle, γ_e. The constant flight path angle is appropriate for steeper initial flight path angle entries for a significant portion of the trajectory where peak heating and deceleration occur. In contrast, we recall that in Yaroshevskii's theory, a small flight path angle assumption is made, given by Eq. (8). Therefore, in principle, this assumption should result in the solution of Yaroshevskii's entry theory to be more accurate than that of Allen–Eggers, especially for shallow initial flight path angles. The accuracy of the new solution to Yaroshevskii's planetary entry equation will be compared with Allen–Eggers solution. The Allen and Eggers theory for planar ballistic entry is briefly summarized as follows.

In Allen–Eggers theory, the velocity can be expressed as a function of the altitude or vice versa. The expression for velocity is given by [3]

$$V = V_0 \exp\left[\frac{SC_D}{2m}\frac{\rho_0}{\beta\sin\gamma_e}\exp(-\beta h)\right] \tag{88}$$

where ρ_0 is the atmospheric density at the planetary surface, V_0 is the entry velocity, and γ_e is the entry flight path angle. Conversely, Eq. (88) can be rearranged to obtain the expression for the altitude of the spacecraft as a function of the spacecraft velocity

$$h = -\frac{1}{\beta}\ln\left[\frac{2m}{SC_D}\frac{\beta\sin\gamma_e}{\rho_0}\ln\left(\frac{V}{V_0}\right)\right] \tag{89}$$

The deceleration of the spacecraft along its trajectory in Earth g's is given by

$$G = \frac{\rho_0 SC_D V_0^2}{2mg}\exp\left[-\beta h + \frac{SC_D}{2m}\frac{\rho_0}{\beta\sin\gamma_e}\exp(-\beta h)\right] \tag{90}$$

The convective stagnation-point heat rate is given by

$$Q_s = \frac{C}{\sqrt{R_n}}V_0^3\exp\left(-\frac{\beta h}{2}\right)\exp\left[\frac{3SC_D}{2m}\frac{\rho_0}{\beta\sin\gamma_e}\exp(-\beta h)\right] \tag{91}$$

8 Simulation Assumptions and Accuracy Assessment

The accuracy of the new analytical solutions is assessed through comparison with the numerically integrated planar equations of motion given by Eqs. (1), (4), and (5). We refer to Sec. 3 for detailed notes related to modeling assumptions and the applicability of the new theory. A MATLAB code was written to numerically integrate the planar equations of motion using the inbuilt ode45 function with relative and absolute tolerances of 10^{-12}. The percentage relative errors, $\%\in_R$, of the approximate analytical solutions are defined by

$$\%\in_R = 100 \times \left|\frac{X_{\text{numerical}} - X_{\text{analytical}}}{X_{\text{numerical}}}\right| \tag{92}$$

where X_* is the numerical or analytical value of the variable being assessed.

In order to take advantage of matrix computations in MATLAB, the length of the vector of variables in the numerical integration and in the analytical propagation must be the same. However, we

recall that to derive Yaroshevskii's equations and to find its solution, the independent variable was changed from time, t, to the velocity variable, x, thereby precluding direct numerical comparison of the numerical and analytical solutions. To surmount this problem, we first numerically integrate the planar equations of motion and use the velocity solution as the independent vector to propagate the approximate analytical solution (using appropriate change of variables wherever required). Therefore, using this approach, individual values of relative error of approximation can be estimated for the length of the velocity vector. Along with the individual values of the relative error, for the conceptual design phase of an entry vehicle, parameters such as peak deceleration, peak heating, altitudes, and velocities at which peak deceleration and heating occur are of paramount interest and are evaluated.

9 Results and Discussion

In this section, we assess the accuracy of the approximate analytical solutions via the relative error defined in Eq. (92). For convenience, we refer to the new approximate analytical solutions as "new analytical" in the figures. We assess the approximate analytical solutions and demonstrate their applicability through the following four ways: (a) a comparison of the new analytical and classical Yaroshevskii solutions with the numerical solution of Yaroshevskii's nonlinear differential equation, Eq. (24); (b) a comparison of first- and second-order new analytical solutions; (c) a comparison of the new analytical and classical Yaroshevskii solutions with the numerical solution in terms of the trajectory variables; and (d) a comparison with the classical Allen–Eggers solution. Three different entry vehicle designs—low, medium, and large ballistic coefficients (B, kg/m^2)—are considered to compare the accuracy of the new analytical solutions and thereafter the entry vehicle medium ballistic coefficient for the other cases. Some physical characteristics of the three entry vehicle are summarized in Table 1. The most relevant parameter in Table 1 for simulation purposes is B. For the strategic case, the ballistic coefficient is assumed to about 20 times that of the Apollo-type entry capsule.

All simulations are performed for entries into Earth's atmosphere. Table 2 summarizes the entry conditions and atmospheric properties of Earth used in the simulation. We assume a strictly exponential model for density where the reference density, ρ_0, is defined at sea level. Unless otherwise stated, throughout the Results and Discussion section, we analyze the analytical solutions for two values of entry flight path angle: (a) shallow, $\gamma_0 = -10$ deg, where the small flight angle approximation is valid, and (b) steep, $\gamma_0 = -70$ deg, where the small flight path angle assumption might induce error.

The accuracy of the analytical solutions is not a direct function of the ballistic coefficient of the entry vehicle but indirectly through how the flight path angle behaves (for different ballistic coefficients) during atmospheric entry. The ballistic coefficient of an entry vehicle is given by

$$B = \frac{m}{SC_D} \tag{93}$$

For circular entry at an arbitrary initial flight path angle, $\gamma_0 = -10$ deg, for the three cases of ballistic coefficients (see Table 1), the percentage relative errors (not plotted) in altitude and flight path angle remain less than 5% for the portion of the trajectory where the key events such as peak deceleration and peak heating occur. Hereafter, the accuracy of the new analytical solutions is assessed for the medium ballistic coefficient case where $B = 360$ kg/m^2 (similar to Apollo-type entry vehicle) for various nonzero entry flight path angles. We also note that throughout the paper, the y-axis title for plots (a) and (b) in figures is the same.

Table 1 Vehicle characteristics with low, medium, and large ballistic coefficients

Spacecraft type	m (kg)	S (m^2)	B (kg/m^2)	R_n (m)	References
Ballutes (low B)	Variable	Variable	10	Variable	[18]
Apollo-type (medium B)	5624	12.03	362	4.69	[19]
Strategic (large B)	Variable	Variable	7200	Variable	

Table 2 Spacecraft entry conditions and atmospheric properties of Earth

Parameters	Value
Earth's radius, km	6378.2
Reference atmospheric density, ρ_0, kg/m^3	1.225
Reference altitude, h_{ref}, km	0
Atmospheric scale height, β^{-1}, km	7.3
βr (average)	900
Initial velocity, V_0, km/s	7.83
Initial altitude, h_0, km	120
Initial flight path angles, γ_0, deg	-10 and -70

9.1 Comparison of the Solutions of Yaroshevskii's Nonlinear Ordinary Differential Equation. Yaroshevskii's second-order nonlinear ordinary differential equation given by Eq. (24) represents the motion of a spacecraft ballistic entry into a planetary atmosphere. At the time of writing this paper, no other known application of the equation form given by Eq. (24) has been found. A perusal of the compendium of nonlinear ordinary differential equations of Sachdev confirms this assessment [20]. Nevertheless, the approximate analytical solution holds mathematical significance.

Both the fourth-order Yaroshevskii's (dashed-dotted) and the second-order new analytical (dashed) solutions are plotted in Fig. 2 by comparing with numerical solution of Eq. (24) for two cases of initial conditions given by the following equations:

$$x_0 = 0; \quad y(0) = 0; \quad y'(0) = 5.235 \tag{94}$$

$$x_0 = 0; \quad y(0) = 0; \quad y'(0) = 36.652 \tag{95}$$

A higher value of the initial slope $y'(0)$ signifies steeper entry flight path angle of the entry spacecraft. We observe that as the initial slope $y'(0)$ is made steeper, the accuracy of the solution increases. The corresponding percentage relative errors for the steeper slope case (Fig. 2(b)) are less than 2% when the value of reaches 3.5, far beyond the critical phases when peak deceleration and peak heating occur. For the small initial slope case, the percent error increases for both the Yaroshevskii's and new analytical solutions for $x > 2$ as shown in Fig. 3. We note that in Figs. 2 and 3, spacecraft entry occurs at the origin.

We are concerned about the accuracy of the solutions when the value of the velocity variable x is small where the critical events during entry occur, such as peak heating and peak deceleration. For the small entry flight path case, the percent relative error in the altitude variable y for both the new analytical and classical Yaroshevskii solutions is less than 5% up to x less than about 2.7. For the large entry flight path angle case, the percent relative errors remain less than 1% throughout.

9.2 Comparison of First- and Second-Order New Analytical Solutions. The first- and second-order new analytical solutions for altitude and flight path angles are given by Eqs. (55) and (57) and Eqs. (60) and (62), respectively. The analytical solutions are suitably transformed into the actual trajectory solutions as outlined in Sec. 6.

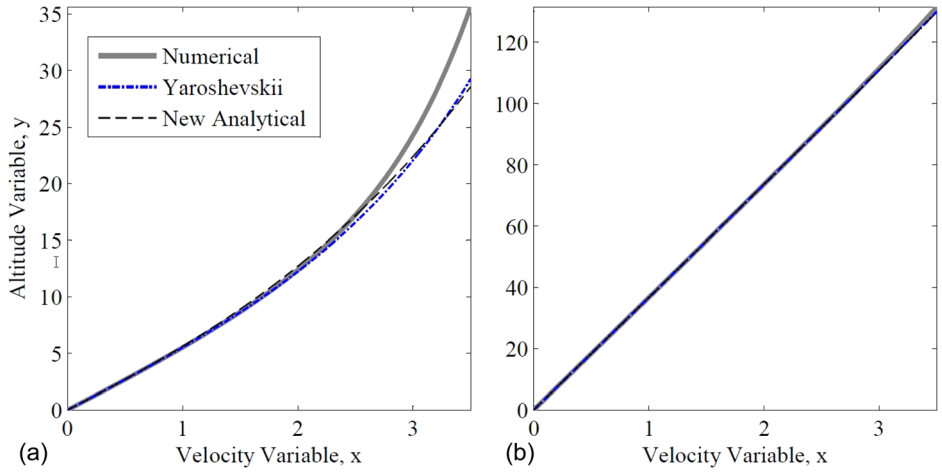

Fig. 2 Comparison of classical Yaroshevskii's, new analytical, and numerical solutions of Yaroshevskii's equation: (*a*) initial conditions in Eq. (94) and (*b*) initial conditions in Eq. (95)

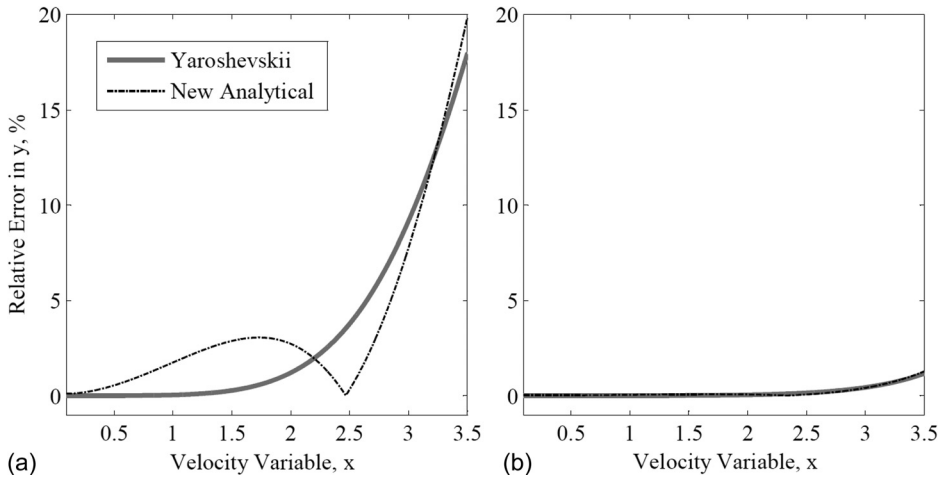

Fig. 3 Comparison of percentage relative errors of the classical Yaroshevskii's and the new analytical solutions: (*a*) initial conditions in Eq. (94) and (*b*) initial conditions in Eq. (95)

We note that both the altitude and flight path angle solutions are simple algebraic functions of the velocity variable, τ. Figure 4 shows the first- and second-order and numerical solutions of altitude as a function of velocity for entry at circular speed for two values of shallow and steeper entry flight path angles. Hereafter, we call $\gamma_0 = -10$ deg as the shallow and $\gamma_0 = -70$ deg as the steep entry flight angles. We observe that the first- and second-order solutions almost overlap, thereby suggesting that the first-order solutions given by Eqs. (55) and (66) are good enough for spacecraft entry studies, and the contribution of the second-order terms in the Poincaré's method of small parameters is not significant. However, the percentage errors of the first- and second-order solutions in altitude can be clearly seen in Fig. 5.

We see that as the initial flight path angle becomes steeper, the difference in first- and second-order diminishes. From Figs. 5(*a*) and 5(*b*), we observe that initially the percent error is high, the reasons of which are twofold: (1) the assumption that the circular speed is given by $\sqrt{gr_0}$ in Eq. (16) is higher than the actual circular speed and (2) only the weighted average value of $\beta r = 900$ is considered to represent the atmospheric density, while in reality the value of βr actually varies from 750 to 1300.

In Fig. 6, the first- and second-order analytical flight path solutions are presented with the numerical values for the shallow and steep initial flight path angle cases. The corresponding percent errors in the analytical solutions are plotted in Fig. 7. It is clear that the percent error in the first-order flight path angle solution for shallow entry flight path angle is higher than the second-order solution. In this case, the first-order solution deviates for $V < 5$ km/s. However, for the steeper initial flight path angle, the first-order solution—which remains fairly constant—is marginally more accurate than the second-order solution in the final portion of the trajectory when the speed becomes small.

From Eqs. (46) and (59), we see that the zero-order flight path angle solution is the constant, b. The magnitude of b is proportional to the magnitude of the flight path angle. We recall that the value of x ranges from 0 (at entry) to around 3.5, and by definition, $\varepsilon\tau$ is equal to x. The most dominant terms due to the first-order (ε) and second-order (ε^2) effects are $(2/b)\varepsilon\tau$ and $-(1/b)(\varepsilon\tau)^2$, respectively. In addition, the value of $\varepsilon\tau$ increases as the entry spacecraft decelerates further. Therefore, at lower speeds, the magnitude of the terms due to the second-order effects is marginally larger than the term due to the first-order effects, i.e., $|-(1/b)(\varepsilon\tau)^2| > |(2/b)\varepsilon\tau|$ and that the two terms have opposite signs. This explains why the error for the second-order solution is marginally larger than the first-order solution as shown in Figs. 6(*a*) and 6(*b*). We also note that the third-order effects are not included in the analysis. Inclusion of third-order effects makes the equations of motion intractable, thereby making it difficult to obtain analytical solutions.

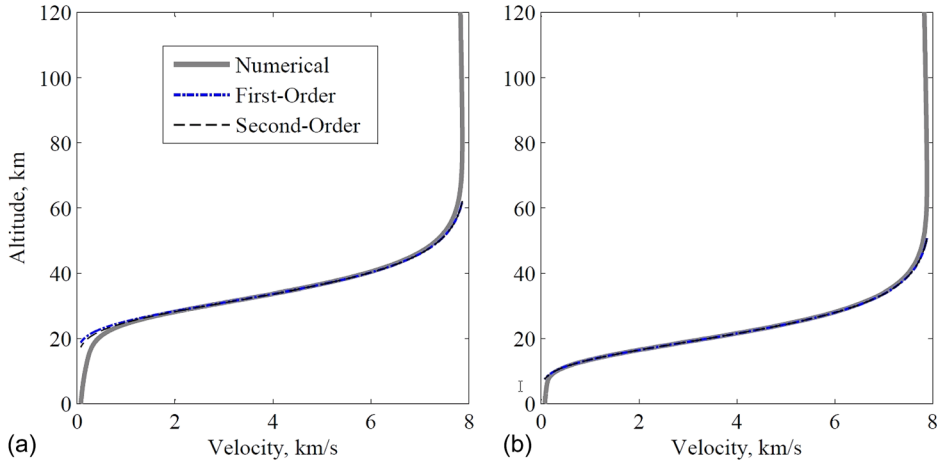

Fig. 4 Comparison of analytical and numerical altitude solutions: (*a*) $\gamma_0 = -10$ deg and (*b*) $\gamma_0 = -70$ deg

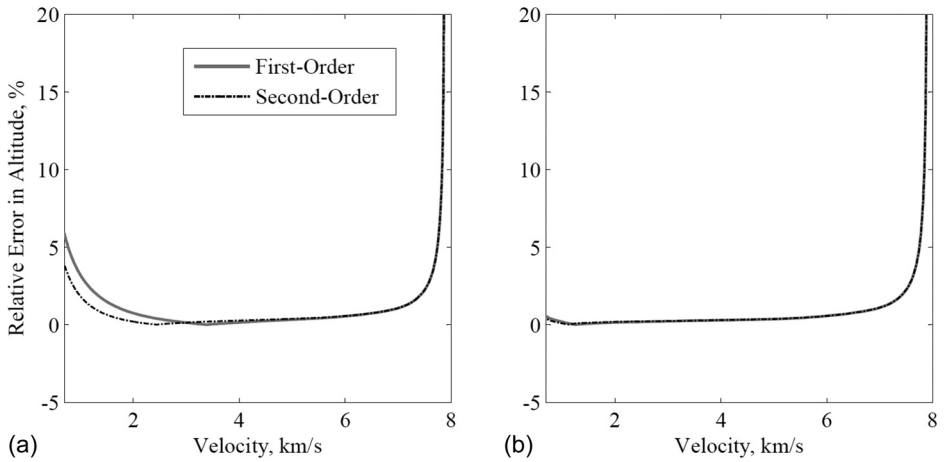

Fig. 5 Comparison of relative error of analytical altitude solutions: (*a*) $\gamma_0 = -10$ deg and (*b*) $\gamma_0 = -70$ deg

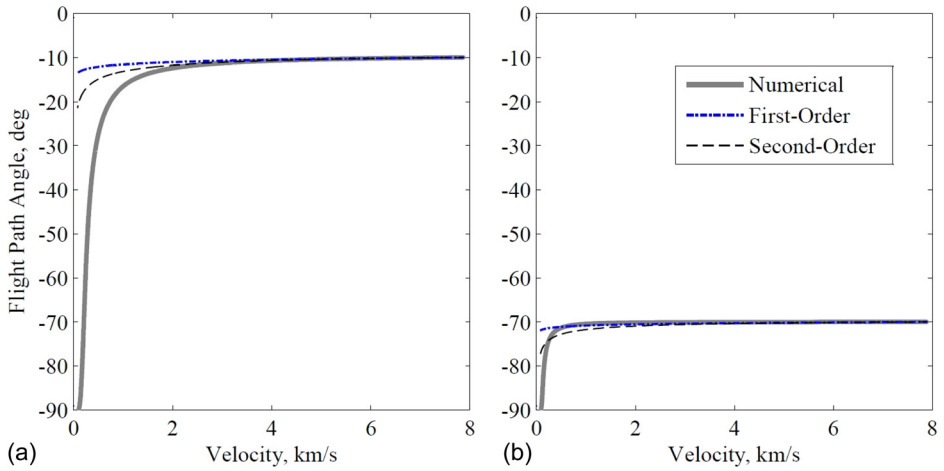

Fig. 6 Comparison of analytical and numerical flight path angle solutions: (*a*) $\gamma_0 = -10$ deg and (*b*) $\gamma_0 = -70$ deg

In this section, we observe that when the percent errors of the analytical altitude and flight path angle solutions are considered, the second-order analytical solutions are more accurate as compared to the first-order solutions for both the shallow and steep entry flight path angles cases. In Sec. 9, we use the second-order new analytical solutions for comparison with the solutions of Yaroshevskii and Allen and Eggers.

Velocity is the independent variable, and therefore, the accuracy of the altitude and flight path angle solutions also determines the accuracy of other parameters such as peak deceleration. Peak

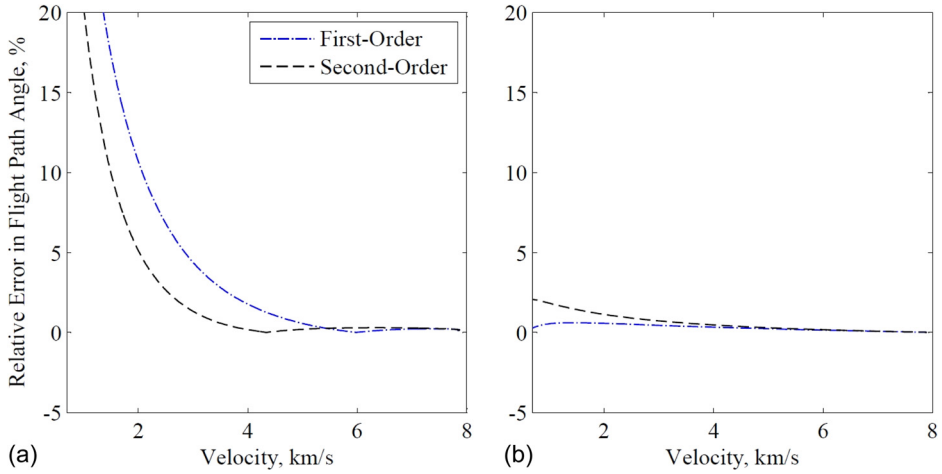

Fig. 7 Comparison of relative error of analytical flight path angle solutions: (*a*) $\gamma_0 = -10$ deg (*b*) $\gamma_0 = -70$ deg

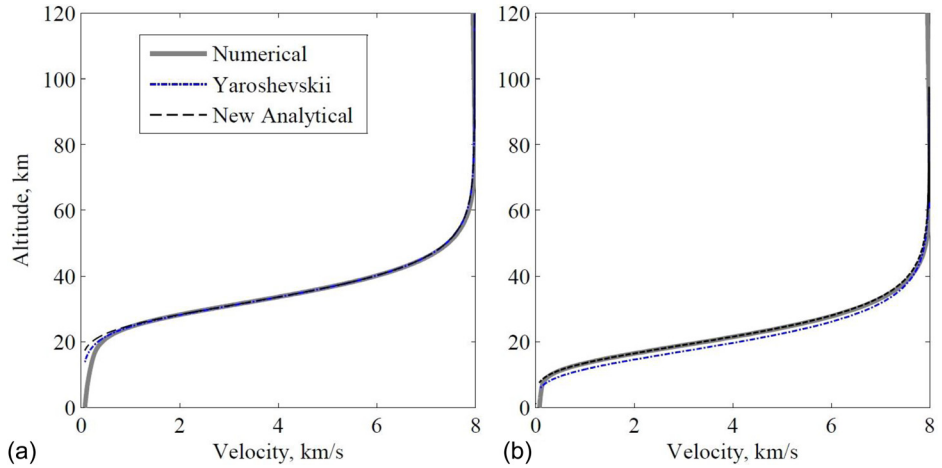

Fig. 8 Comparison of analytical, classical Yaroshevskii's, and numerical altitude solutions: (*a*) $\gamma_0 = -10$ deg (*b*) $\gamma_0 = -70$ deg

deceleration and peak convective stagnation-point heating rate are two other key parameters in the design of entry spacecraft. In Secs. 9.3 and 9.4, the accuracy of the analytical deceleration and stagnation-point heating rate analytical solutions will be assessed.

9.3 Comparison of the New Analytical Solution With the Classical Yaroshevskii Solution. We recall that for circular entry at nonzero initial flight path angles, Yaroshevskii found series solutions of the altitude variable y in terms of the velocity variable x. The altitude and flight path angle variable solutions are given by Eqs. (28)–(36) and we retained a solution of the order 5 in x. On the other hand, for the new analytical solution, we retain terms up to order 2 only.

The fifth-order classical Yaroshevskii's and second-order new analytical solutions for altitude are shown in Fig. 8 for the shallow and steep entry flight angle cases. For the shallow flight path angle case, both Yaroshevskii's and the new analytical solutions show good agreement; however, for the steep flight path angle, the error in Yaroshevskii's solution is noticeable. The corresponding percent relative errors for the shallow and steep entry flight path angles are shown in Fig. 9. For the shallow flight path angle case, the percent error for both the Yaroshevskii's solutions and the new analytical solution is similar (of the order 1% or less). For velocities less than 1.4 km/s, the percent error of the new analytical solution increases as compared to Yaroshevskii's solution. However, the efficacy of the new analytical solution for altitude becomes clear by observing the percent error for the steep flight path angle case in Fig. 9(*b*). While the percent error of Yaroshevskii's solution continually increases to around 15% when the velocity reduces to around 1.4 km/s, the percent error for the new analytical solution remains steady or decreases throughout the trajectory.

Similarly, the fifth-order classical Yaroshevskii and new second-order analytical flight path angle solutions are plotted in Fig. 10, and the corresponding percent errors are plotted in Fig. 11. For shallow flight path angle case (Figs. 10(*a*) and 11(*a*)), clearly Yaroshevskii's solution is better for most part of the trajectory when the velocity is greater than 1.9 km/s and the percent error remains less than 2% after which it increases. On the other hand, the percent error of the new analytical solution, for velocities greater than 3 km/s, is equal to or less than that of Yaroshevskii's, but increases exponentially thereafter. At the same time, for the steeper flight path angle case, the percent errors (as shown in Fig. 11(*b*)) for both Yaroshevskii's and the new analytical solution remain fairly small and increase to around 3% when the velocity reduces to less than 1 km/s.

The peak deceleration, altitude, and velocity at which the peak deceleration occurs are very important parameters in the design of an entry spacecraft. An entry spacecraft should be able to withstand the deceleration loads. The deceleration profile for the

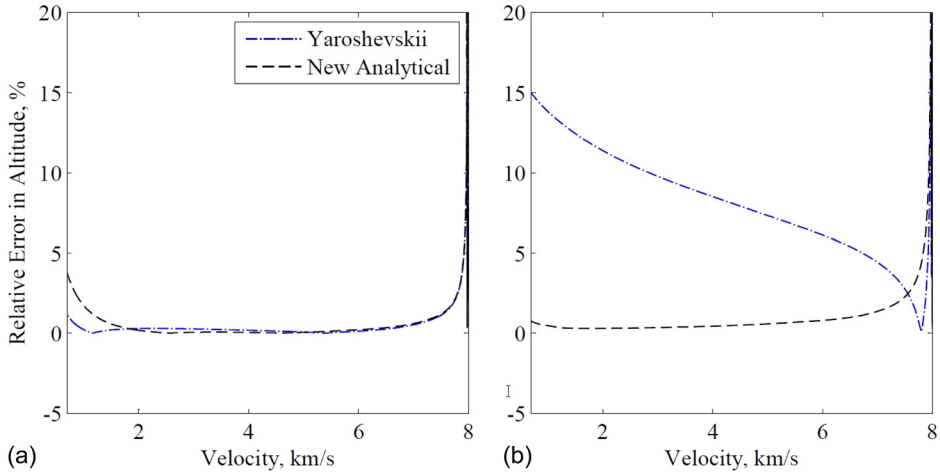

Fig. 9 Comparison of percentage relative errors of the altitude solutions: (*a*) $\gamma_0 = -10$ deg (*b*) $\gamma_0 = -70$ deg

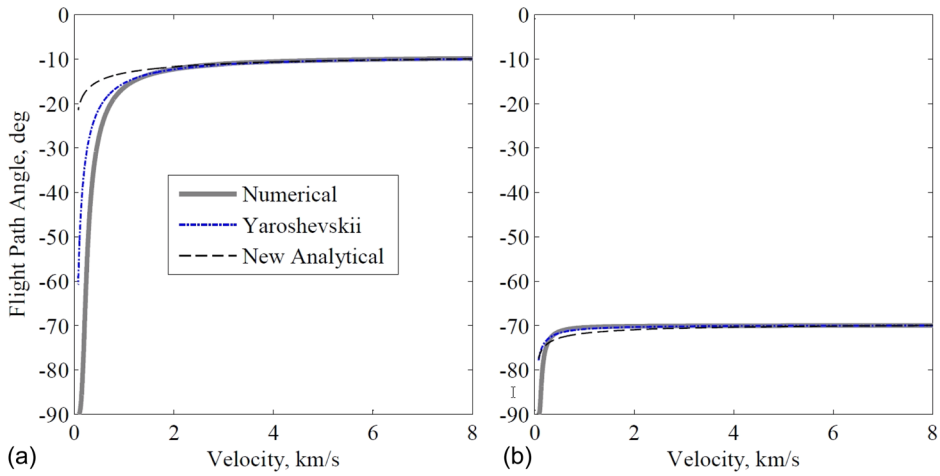

Fig. 10 Comparison of percentage relative errors of the altitude solutions: (*a*) $\gamma_0 = -10$ deg and (*b*) $\gamma_0 = -70$ deg

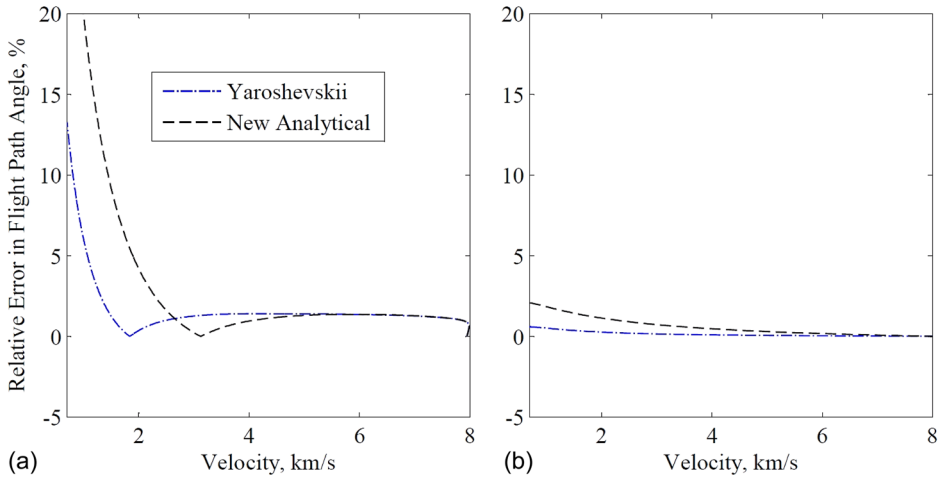

Fig. 11 Comparison of percentage relative errors of the flight path angle solutions: (*a*) $\gamma_0 = -10$ deg and (*b*) $\gamma_0 = -70$ deg

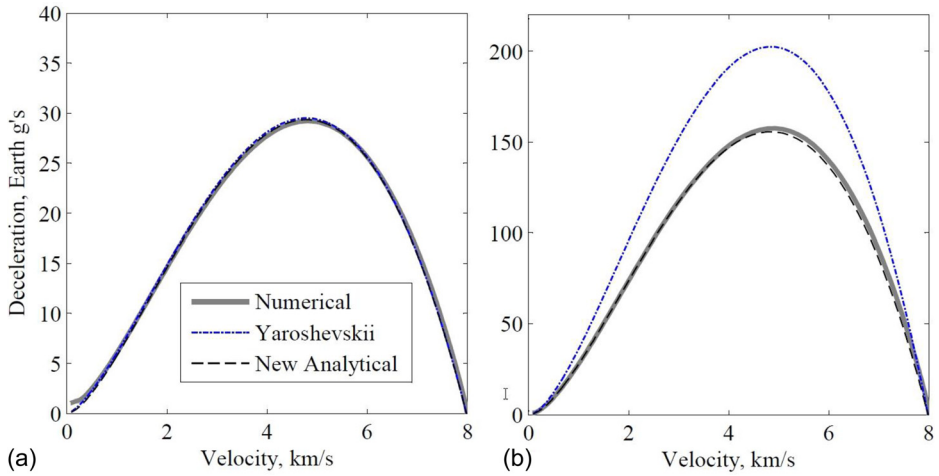

Fig. 12 Comparison of analytical, classical Yaroshevskii's, and numerical deceleration solutions: (*a*) $\gamma_0 = -10$ deg and (*b*) $\gamma_0 = -70$ deg

Table 3 Comparison of the peak deceleration, altitude at peak deceleration, and relative errors

Entry γ_i (deg)	$G^n_{\max}$	h at $G^n_{\max}$ (km)	$\%\in_R$, $G^Y_{\max}$	$\%\in_R$, $G^A_{\max}$	$\%\in_R$, h at $G^Y_{\max}$	$\%\in_R$, h at $G^A_{\max}$
−10	29.2	35.9	1.0	0.5	0.3	0.2
−70	157.5	24.0	28.4	1.2	7.6	0.5

shallow and steeper entry flight path angles is shown in Fig. 12. For the shallow flight path angle, Yaroshevskii's and new analytical deceleration solutions overlap each other. Unlike the previous cases, where we analyzed the pointwise percent error, we are more interested in the peak values, velocity, and the altitude at which peak deceleration occurs, as well as respective relative errors.

For the shallow and steep entry flight path angle cases, the numerical values of deceleration, altitude at peak deceleration, and the percent errors of the corresponding analytical values from Yaroshevskii's and the new solution are summarized in Table 3. Clearly, the estimates of peak deceleration and the altitude at peak deceleration using the new analytical solution are better than those using Yaroshevskii's solution. In fact for the steeper entry flight path angle, the percent relative error of the peak deceleration using Yaroshevskii is as high as 28%, as opposed to just 1.2% using the new analytical solution. The percent relative errors for peak deceleration and altitude at peak deceleration using the new analytical solution range between a minimum of 0.2% and a maximum of 1.2%. While it is mentioned in Table 3, the percent relative errors in the velocity at which peak deceleration occurs are about 1% for both Yaroshevskii's and new analytical solutions.

Similarly, the numerical, Yaroshevskii, and new analytical solutions of the convective stagnation-point heating rate are plotted in Fig. 13 for the shallow and steep flight path angle cases. For the shallow flight path angle, Yaroshevskii's and the new analytical solutions for stagnation-point heating rate (referred to as heating rate henceforth) almost overlap.

However, for the steeper flight path angle, the percent error in Yaroshevskii's solution for stagnation-point heating rate is conspicuously large as compared to the new analytical solution. The numerical values of the peak heating, altitude at peak deceleration, and percent errors of the corresponding analytical values from Yaroshevskii's and the new solution are summarized in Table 4. The percent errors in the estimation of heating rate using Yaroshevskii's solution range from a minimum of 2.8% (for shallow entry) to a maximum of 16.2% (for steeper entry). The corresponding percent errors using the new analytical solution are 2.6% and 1.9%, respectively.

A more detailed history of percent relative error in the classical Yaroshevskii and new analytical solutions for convective stagnation-point heat rate is shown in Fig. 14. The percent relative

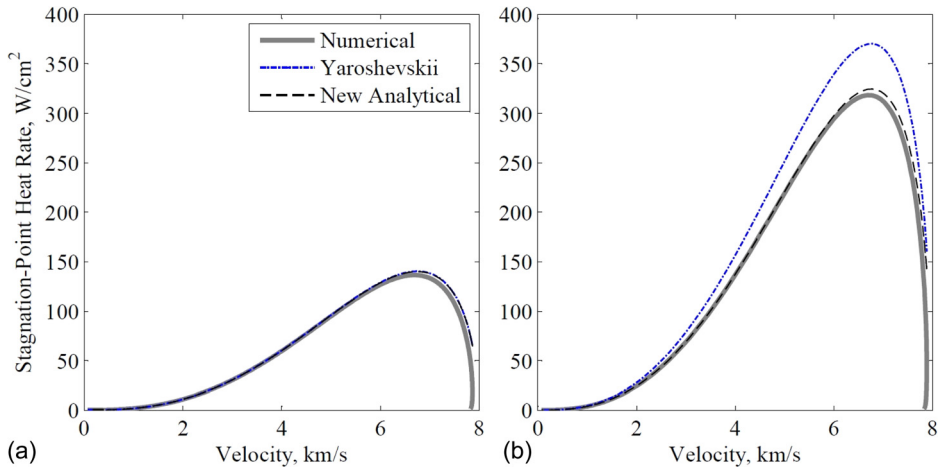

Fig. 13 Comparison of analytical, classical Yaroshevskii's, and numerical stagnation-point heat rate solutions: (*a*) $\gamma_0 = -10$ deg and (*b*) $\gamma_0 = -70$ deg

Table 4 Comparison of the peak stagnation-point heat rate, altitude at peak deceleration, and relative errors

Entry γ_i (deg)	$Q^n_{s,\max}$	h at $Q^n_{s,\max}$	$\%\in_R$, $Q^Y_{s,\max}$	$\%\in_R$, $Q^A_{s,\max}$	$\%\in_R$, h at $Q^Y_{s,\max}$	$\%\in_R$, h at $Q^A_{s,\max}$
−10	136.6	43.4	2.8	2.6	1.7	1.7
−70	318.7	31.1	16.2	1.9	3.8	2.3

errors for the shallow entry case are comparable for both the classical Yaroshevskii's and new analytical solutions. However, for steeper entry, the percent error in stagnation-point heating rate for Yaroshevskii solution is consistently greater than 14%.

Based on the previous discussion, we observe that the new analytical solutions are more accurate than the classical solutions in estimating key trajectory parameters such as peak deceleration, peak convective stagnation-point heating rate, and the corresponding altitudes. Not only are the new analytical solutions accurate but also they extend the applicability of Yaroshevskii's entry theory to steeper entry flight angles.

We found that the classical Yaroshevskii solution applies for ballistic entry at circular speed for a range of entry flight path angle, $-40\,\text{deg} \le \gamma_0 \le -5\,\text{deg}$. If the entry flight path angle is made steeper than −40 deg, the error in the classical Yaroshevskii solution increases to unacceptable levels. However, the new analytical solution extends the applicability of the Yaroshevskii entry equation to cover almost the entire range of entry flight path angle, $-90\,\text{deg} \le \gamma_0 \le -5\,\text{deg}$.

9.4 Comparison of the New Analytical Solution With the Classical Allen–Eggers Solutions. As outlined in Sec. 7, two of the most important simplifying assumptions for the Allen–Eggers solution for planar ballistic entry are that the tangential gravitational acceleration, $g \sin\gamma$, is negligible and that the flight path angle is considered as constant. Clearly, Yaroshevskii's theory is comparatively more sophisticated than that of Allen and Eggers, as a small flight path angle approximation is used in the former.

Therefore, it follows that the error in the Allen and Eggers solution as compared to numerical solution is larger than those associated with the new analytical solution (outlined in Sec. 9.3). In contrast to the results in Secs. 9.2 and 9.3, the plots are for entry at circular speed for entry flight angles, $\gamma_0 = -5\,\text{deg}$ (shallow) and $\gamma_0 = -70\,\text{deg}$ (steeper). We note that the shallow entry flight path angle is changed from $\gamma_0 = -10\,\text{deg}$ in Secs. 9.2 and 9.3 to $\gamma_0 = -5\,\text{deg}$.

The numerical, Allen and Eggers, and the new analytical altitude solutions are plotted for the shallow and steeper entry cases in Fig. 15. The discrepancy between the Allen–Eggers and

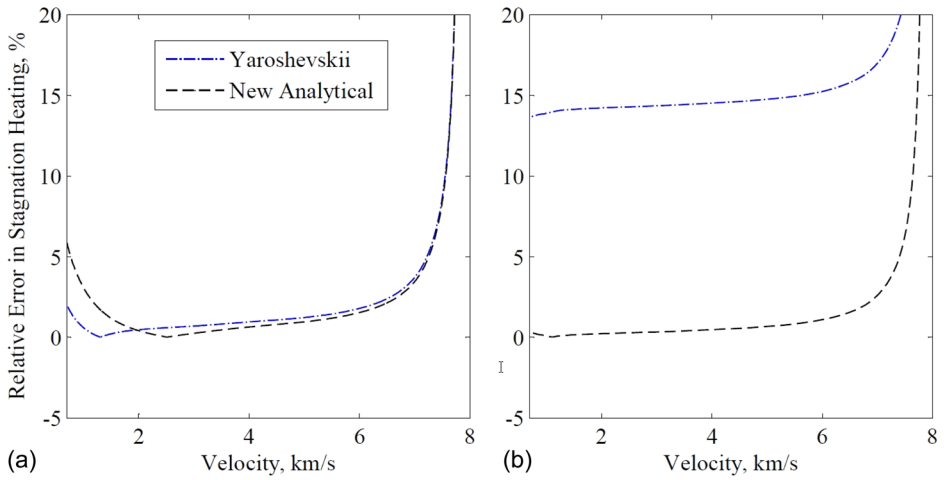

Fig. 14 Comparison of analytical, classical Yaroshevskii's, and numerical stagnation-point heat rate solutions: (*a*) $\gamma_0 = -10\,\text{deg}$ and (*b*) $\gamma_0 = -70\,\text{deg}$

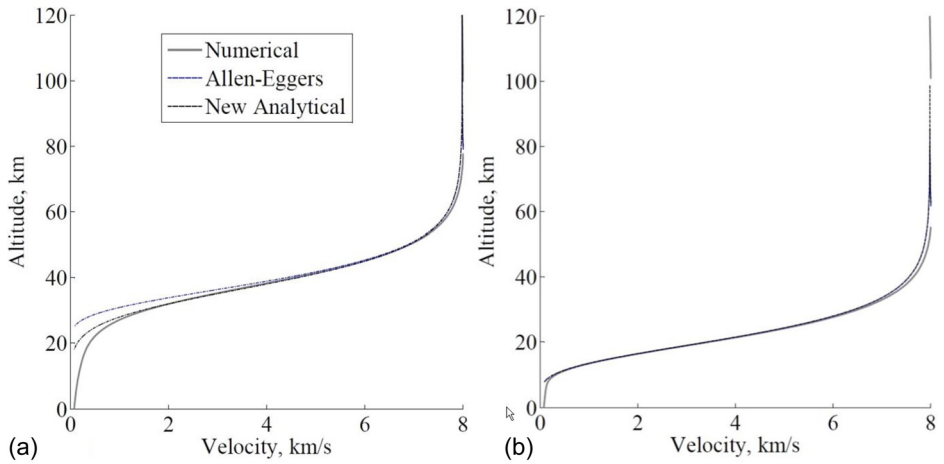

Fig. 15 Comparison of analytical, classical Allen–Eggers, and numerical altitude solutions: (*a*) $\gamma_0 = -5\,\text{deg}$ (*b*) $\gamma_0 = -70\,\text{deg}$

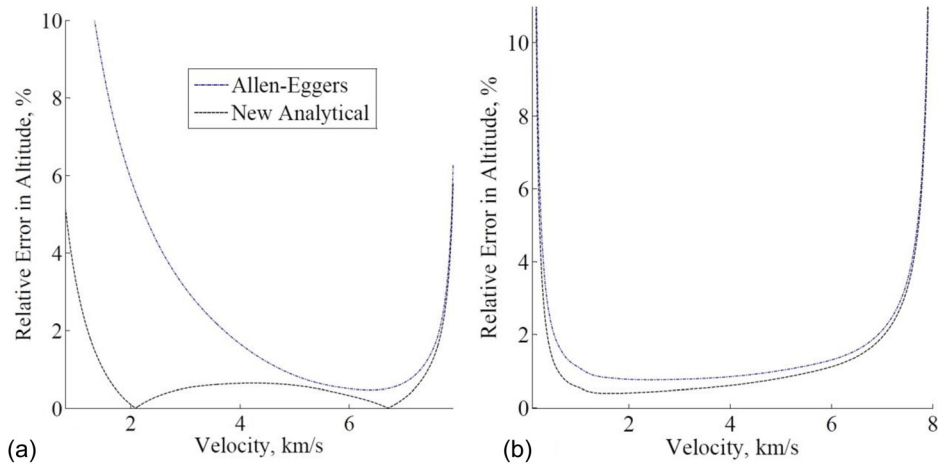

Fig. 16 Comparison of percentage relative errors of the altitude solutions: (*a*) $\gamma_0 = -5$ deg (*b*) $\gamma_0 = -70$ deg

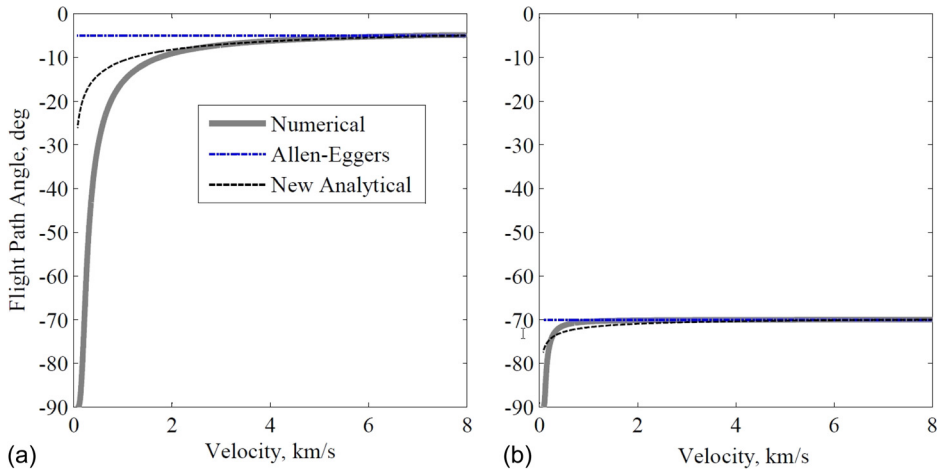

Fig. 17 Comparison of analytical, classical Allen–Eggers, and numerical flight path angle solutions: (*a*) $\gamma_0 = -5$ deg and (*b*) $\gamma_0 = -70$ deg

numerical solutions is evident for the latter part of the trajectory when the velocity is small (<4 km/s). For the steep entry flight path angle case, we observe from Fig. 15(*b*) that the difference (the absolute error) between the Allen–Eggers and numerical solutions remains fairly constant, which means that the percent relative error should increase as the velocity decreases. We observe this trend in the plots of percent relative error of the Allen–Eggers and new analytical solutions as shown in Fig. 16.

For the small flight path angle case, the average percent relative error in altitude for the Allen–Eggers solution is small (<2%) initially and increases exponentially to 10% as the velocity decreases to around 1 km/s. The corresponding error for the new analytical solutions is small (<1%), and the error increases when the velocity becomes less than 2 km/s. As the accuracy of the new analytical solution for altitude improves for the steep entry flight path angle case, the percent error of Allen–Eggers solution is also similar as shown in Fig. 16(*b*).

Figure 17 shows the numerical, Allen–Eggers, and new analytical flight path angle solutions for the two cases of entry flight path angle. The percent relative error in the Allen–Eggers and new analytical solutions is shown in Fig. 18. We recall that the Allen–Eggers solution assumes a constant flight path angle approximation at the initial value at the entry interface. For the steep entry flight path angle case, the constant flight path angle approximation holds true as the nature of entry is that for large entry flight path angles. For an entry spacecraft, the flight path angle remains constant for a significant portion of the trajectory. Therefore, the percent error in the flight path angle solution of Allen–Eggers is marginally less compared to the new analytical solution (see Figs. 17(*b*) and 18(*b*)). On the other hand, for the shallow entry flight path angle case, the percent error in the Allen–Eggers flight path angle solution increases rapidly.

Finally, the numerical, Allen–Eggers, and new analytical solutions for deceleration are plotted in Fig. 19. The discrepancy between the numerical and the Allen–Eggers deceleration solutions is visually apparent. The numerical values of the peak deceleration, percent relative errors of the Allen–Eggers and the new analytical solutions for peak deceleration, as well as the altitude at peak deceleration are summarized in Table 5.

In contrast to estimates of peak deceleration using the classical Yaroshevskii solution, Allen and Eggers' estimates are actually better. The percent relative error in peak deceleration using Allen–Eggers is high at 5.4% for the shallow entry case and low at 3.1% for the steep entry case. Similarly, the percent relative error in altitude at peak deceleration using Allen–Eggers is high at 2.7% for the shallow entry case and low at 1.0% for the steep entry case. Of course, in all the cases, the percent relative errors using new analytical solutions are comparatively lower.

For the shallow entry case, the percent relative error in the velocity at peak deceleration is about 24% and that for the steeper

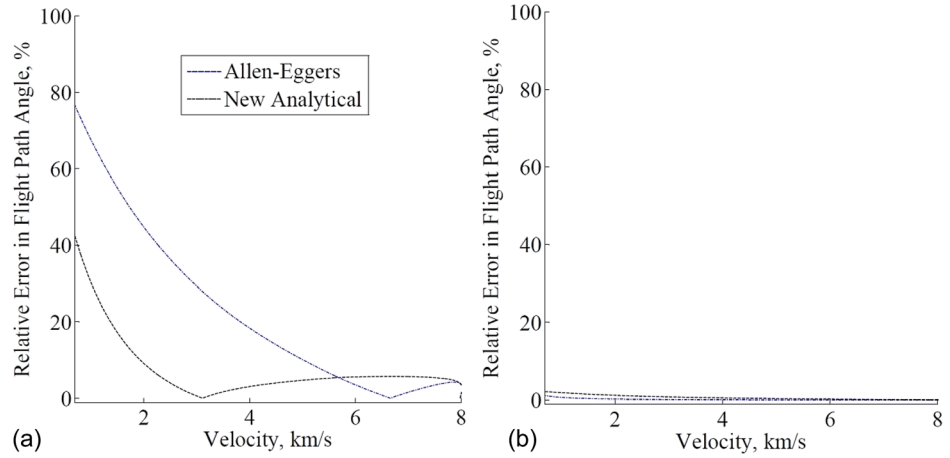

Fig. 18 Comparison of percentage relative errors of the flight path angle solutions: (*a*) $\gamma_0 = -5$ deg and (*b*) $\gamma_0 = -70$ deg

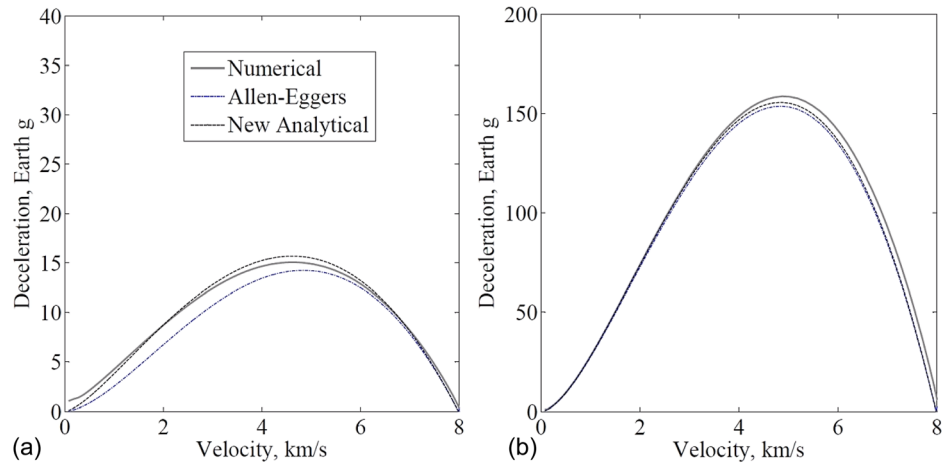

Fig. 19 Comparison of analytical, classical Allen–Eggers, and numerical deceleration solutions: (*a*) $\gamma_0 = -5$ deg and (*b*) $\gamma_0 = -70$ deg

Table 5 Comparison of the numerical and analytical values of peak deceleration, altitude at peak deceleration, and relative errors

Entry γ_i (deg)	$G^n_{\max}$	h at $G^n_{\max}$ (km)	$\%\in_R$, $G^{AE}_{\max}$	$\%\in_R$, $G^{A}_{\max}$	$\%\in_R$, h at $G^{EG}_{\max}$	$\%\in_R$, h at $G^{A}_{\max}$
−5	15.2	40.1	5.4	2.6	2.7	0.4
−70	157.5	24.0	3.1	1.2	1.2	0.5

entry case is about 19%, respectively. We recall that from the previous subsection that the percent relative error in the velocity at peak deceleration using both the classical Yaroshevskii and new analytical solutions is about 1%.

10 Conclusion

Based on prior analytic work by Yaroshevskii and Vinh, we found a new approximate analytical solution of Yaroshevskii's second-order nonlinear ordinary differential equation that represents the planar ballistic entry of spacecraft into planetary atmospheres at circular speed and nonzero entry flight path angles. We note that the solution has a singularity when the entry flight path angle is zero; however, such a case has very limited applicability. Poincaré's method of small parameters is used to solve Yaroshevskii's equation to find the first- and second-order perturbative solutions. We have found approximate analytical expressions for the altitude and flight path angle of a spacecraft entering a planetary atmosphere as a function of its velocity. Consequently, expressions for important trajectory parameters such as deceleration, stagnation-point heat rate, and load are obtained. We demonstrate that the accuracy of the first-order solution is in fact similar to that of the second-order approximate analytical solution. We also found that the new analytical solution is more accurate than the classical Yaroshevskii solution for a range of shallow to steep entry flight path angles. The estimates of peak deceleration and the altitude at peak deceleration using the new analytical solution are better than those obtained using Yaroshevskii's solution. In fact, for steeper entry flight path angle, the percent relative error of the peak deceleration using Yaroshevskii is an order of magnitude larger than the new analytical solution.

The new analytical solution extends the applicability of the Yaroshevskii entry equation for any nonzero entry flight path angle from a shallow value of $\gamma_0 = -3$ deg to up to the steepest case when $\gamma_0 = -90$ deg. The comparison of the new analytical solutions with the classical Allen–Eggers solution showed the superiority of the new results. The new approximate solution is the second known solution to Yaroshevskii's planetary entry equation and will add to the repertoire of classical approximate analytical solutions for the planar ballistic entry of a spacecraft into planetary atmospheres. Though it is not the part of the analysis presented, the solutions may help in rapid conceptual probe mission studies for the exploration of the solar system. In addition, the

solution can provide initial guesses for the optimization subroutines used to solve spacecraft entry problems.

Acknowledgment

Some results included in this paper were first presented at the American Astronautical Society (AAS)/American Institute of Aeronautics and Astronautics (AIAA) Astrodynamics Specialist Conference, Hilton Head, SC, Aug. 11–15, 2013.

Nomenclature

A = variables with superscript "A" are values from the new analytical solution
AE = variables with superscript "AE" are values from Allen–Eggers' solution
B = ballistic coefficient of spacecraft, kg/m^2
C = stagnation-point heating coefficient, kg$^{1/2}$ m^{-1}
C_D = drag coefficient of entry spacecraft
C_F = acceleration due to gravity of the planet, m/s^2
C_L = lift coefficient of entry spacecraft
G = deceleration of an entry vehicle, Earth g's
$G_{\max}$ = peak deceleration of the entry vehicle, Earth g's
gr = circular speed squared, m^2/s^2
h_{ref} = reference altitude at which the reference atmospheric density is defined, km
m = entry vehicle mass, kg
n = variables with superscript "n" are values from numerical solution
Q_s = stagnation-point heat rate, W/m^2 or W/cm^2
$Q_{s,\max}$ = peak stagnation-point heat rate, W/m^2 or W/cm^2
Q_t = stagnation-point integrated heat load, J/cm^2
r = radial distance of the spacecraft from the center of a planetary body, m or km
r_{planet} = radius of the planet, m or km
r_0 = radial distance of the spacecraft at the entry interface, m or km
R_n = nose radius of the entry spacecraft, m or km
s = distance traveled by spacecraft in a planetary atmosphere, rad
S = entry vehicle reference area, m^2
V = spacecraft velocity, m/s or km/s
$\bar{V}$ = velocity, dimensionless
x = velocity, dimensionless
y = altitude, dimensionless
Y = variables with superscript "Y" are values from Yaroshevskii's solution
0 = variables with subscript "0" are initial values
β = inverse of atmospheric scale height, m^{-1} or km^{-1}
βr = Chapman's atmospheric planetary parameter
γ = flight path angle, deg
γ_0 = entry (initial) flight path angle, deg
ε = a small parameter
$\in_R$ = relative error of a variable
η = modified altitude variable
θ = longitude, deg
ρ = atmospheric density, kg/m^3
σ = bank angle of the spacecraft, deg
τ = velocity variable, dimensionless
ϕ = latitude, deg
ψ = heading angle, deg
Ω = longitude of the ascending node, deg

References

[1] Sänger, E., and Bredt, J., 1994, "A Rocket Drive for Long Range Bombers," Translated by M. Hamermesh, Technical Information Branch, Navy Department, Santa Barbara, CA, Report No. CGD-32.
[2] Gazley, C., 1957, "Deceleration and Heating of a Body Entering a Planetary Atmosphere From Space," RAND Corporation, Santa Monica, CA, Report No. P-955.
[3] Allen, H. J., and Eggers, A. J., 1958, "A Study of the Motion and Aerodynamic Heating of Ballistic Missiles Entering the Earth's Atmosphere at High Supersonic Speeds," National Advisory Committee for Aeronautics, Moffett Field, CA, Report No. NACA-TR-1381.
[4] Loh, W. H. T., 1963, *Dynamics and Thermodynamics of Planetary Entry*, Prentice-Hall, Englewood Cliffs, NJ.
[5] Loh, W. H. T., 1968, *Re-Entry and Planetary Entry Physics and Technology: I—Dynamics, Physics, Radiation, Heat Transfer and Ablation*, Springer-Verlag, New York.
[6] Loh, W. H. T., 1962, "A Second-Order Theory of Entry Mechanics Into a Planetary Atmosphere," J. Aerosp. Sci., **29**(10), pp. 1210–1221.
[7] Chapman, D. R., 1959, "An Approximate Analytical Method for Studying Entry Into Planetary Atmospheres," NASA, Washington, DC, Technical Report No. R-11.
[8] Longuski, J. M., and Saikia, S. J., 2013, "Analytical Theory for Ballistic Entry Into Planetary Atmosphere at Circular Speed for Various Flight Path Angles," AAS/AIAA Astrodynamics Specialist Conference, Hilton Head, SC, Aug. 11–15, pp. 4–8.
[9] Longuski, J. M., and Saikia, S. J., 2013, "Analytical Theory for Ballistic Spacecraft Planetary Entry at Moderate and Large Entry Flight Path Angles," AAS/AIAA Astrodynamics Specialist Conference, Hilton Head, SC, Aug. 11–15, pp. 5–15.
[10] Longuski, J. M., 1979, "Analytic Theory of Orbit Contraction and Ballistic Entry Into Planetary Atmospheres," Ph. D. thesis, The University of Michigan, Ann Arbor, MI.
[11] Longuski, J. M., and Vinh, N. X., 1980, "Analytic Theory of Orbit Contraction and Ballistic Entry Into Planetary Atmospheres," Jet Propulsion Laboratory, Pasadena, CA, Report No. 80-58.
[12] Vinh, N. X., Busemann, A., and Culp, R. D., 1980, *Hypersonic and Planetary Entry Flight Mechanics*, The University of Michigan Press, Ann Arbor, MI.
[13] Vinh, N. X., and Brace, F. C., 1974, "Qualitative and Quantitative Analysis of the Exact Atmospheric Entry Equations Using Chapman's Variables," XXVth Congress of the International Astronautical Federation, Amsterdam, The Netherlands, Sept. 30–Oct. 5, Paper No. 74-010, pp. 36–38.
[14] Brace, F. C., 1974, "An Improved Chapman Theory for Studying Entry Into Planetary Atmospheres," Ph.D. thesis, The University of Michigan, Ann Arbor, MI.
[15] Blestos, N. A., 1976, "Performance and Control With Lift Modulation of Hypervelocity Entry Vehicles," Ph.D. thesis, The University of Michigan, Ann Arbor, MI.
[16] Yaroshevskii, V. A., 1964, "The Approximate Calculation of Trajectories of Entry Into the Atmosphere I," Kosm. Issled., **2**(4), pp. 507–531.
[17] Yaroshevskii, V. A., 1964, "The Approximate Calculation of Trajectories of Entry Into the Atmosphere II," Kosm. Issled., **2**(5), pp. 508–528.
[18] Gates, K. L., and Longuski, J. M., 2010, "Aerocapture Ballutes Versus Aerocapture Tethers for Exploration of the Solar System," J. Spacecr. Rockets, **47**(4), pp. 590–596.
[19] Crowder, R. S., and Moote, J. D., 1969, "Apollo Entry Aerodynamics," J. Spacecr. Rockets, **6**(302–307), pp. 302–307.
[20] Sachdev, P. L., 1997, *A Compendium on Nonlinear Ordinary Differential Equations*, Wiley, New York.